Lawrence Berkeley National Laboratory
LBL Publications

Computing Free Energies with Fluctuation Relations on Quantum Computers

Lindsay Bassman Oftelie,[1, *] Katherine Klymko,[1] Diyi Liu,[2] Norm M. Tubman,[3] and Wibe A. de Jong[1]

[1] *Lawrence Berkeley National Lab, Berkeley, California, USA 94720*
[2] *School of Mathematics, University of Minnesota, Minnesota, USA 55455*
[3] *NASA Ames Research Center, Mountain View, California, USA 94035*

As a central thermodynamic property, free energy enables the calculation of virtually any equilibrium property of a physical system, allowing for the construction of phase diagrams and predictions about transport, chemical reactions, and biological processes. Thus, methods for efficiently computing free energies, which in general is a difficult problem, are of great interest to broad areas of physics and the natural sciences. The majority of techniques for computing free energies target classical systems, leaving the computation of free energies in quantum systems less explored. Recently developed *fluctuation relations* enable the computation of free energy differences in quantum systems from an ensemble of dynamic simulations. While performing such simulations is exponentially hard on classical computers, quantum computers can efficiently simulate the dynamics of quantum systems. Here, we present an algorithm utilizing a fluctuation relation known as the Jarzynski equality to approximate free energy differences of quantum systems on a quantum computer. We discuss under which conditions our approximation becomes exact, and under which conditions it serves as a strict upper bound. Furthermore, we successfully demonstrate a proof-of-concept of our algorithm using the transverse field Ising model on a real quantum processor. As quantum hardware continues to improve, we anticipate that our algorithm will enable computation of free energy differences for a wide range of quantum systems useful across the natural sciences.

Introduction.–Free energy is a central thermodynamic property used to compute virtually all equilibrium properties of a physical system [1]. Broadly useful across the natural sciences, free energy differences are employed in the construction of phase diagrams [2–5], the prediction of transport properties and reaction constants [6], and the calculation of protein-ligand binding affinities required for computer-aided drug design [7–11]. In general, computing free energy differences is a difficult problem due to the challenges in adequately sampling the important configurations of a system [1]. As such, a great deal of research has focused on developing techniques for calculating free energy differences [1, 12–16]. The majority of techniques have been developed for classical systems; less well-studied are methods for computing free energy differences in quantum systems [6, 17–19] (see Section I in the Supplemental Information (SI) [20], which includes Refs. [21–24]).

In general, extending thermodynamics to the quantum realm is non-trivial, as its theoretical constructs tend to focus on bulk properties of macroscopic-size systems derived from averages over a very large number of constituent particles. An implicit assumption here is that individual deviations from the average become practically insignificant, allowing thermodynamics to make predictions about systems without detailed knowledge of the microscopic constituents. However, as the size of the system begins to shrink, these deviations, originating from thermal motion (and possibly quantum effects), become more appreciable. Rather surprisingly, these deviations, or fluctuations, satisfy some profound equalities, generally referred to as fluctuation relations (FRs) [25, 26].

FRs relate fluctuations in non-equilibrium processes to equilibrium properties like free energy differences.

Arguably the most celebrated FR is the Jarzynski equality [27, 28], in which the free energy difference between two equilibrium states is derived from an exponential average over an ensemble of measurements of the work required to drive the system from one state to the other. While the Jarzynski equality has proven important theoretically, providing one of the few strong statements that can be made about non-equilibrium systems, its utility for computing free energies of quantum systems has thus far been limited. This is because simulating the exact trajectories of quantum systems on classical computers requires resources that scale exponentially with system size. Therefore, computing even a single trajectory of a quantum system with tens of particles can quickly become intractable on classical computers, let alone an ensemble of trajectories.

One potential path forward for computing this ensemble of trajectories is to employ quantum computers, which were proven capable of efficiently simulating the dynamics of quantum systems over two decades ago [29–32]. A plethora of recent work has successfully demonstrated dynamic simulations of the Hubbard model [33], the Schwinger model [34], and various spin models [35–40] on currently available quantum hardware, while further work has shown how such dynamic simulations can be used to compute various static properties such as cross-sections in inelastic neutron scattering [41], magnon spectra [42], and transport properties [43].

Here, we present an algorithm to approximate free energy differences using the Jarzynski equality based on dynamic simulations performed on a quantum computer. We discuss under which conditions the approximation becomes exact and under which conditions the approxi-

* Corresponding author. lbassman@lbl.gov

mation gives a strict upper bound, which is tighter than the usual upper bound given by the reversible work theorem. We provide a proof-of-concept demonstration for our algorithm by computing free energy differences in a transverse field Ising model (TFIM) on a real quantum processor. Further improvements in quantum circuit generation [44–47], error mitigation techniques [48, 49], and quantum hardware [50] will enable our algorithm to compute free energy differences for scientifically relevant systems on quantum computers in the near-future (see Section II of the SI, which includes Refs. [51–57]). Our algorithm demonstrates how quantum computers, with their ability to efficiently perform dynamic simulations of quantum systems, provide an unprecedented platform for computing free energy differences.

Theoretical background and framework.– Initially derived and experimentally verified for classical systems [58–63], the Jarzynski equality has since been extended to both closed [25, 26, 64–68] and open [69–77] quantum systems, theoretically. Experimental verification of the Jarzynski equality in closed quantum systems was proposed [78] and later demonstrated with a liquid-state nuclear magnetic resonance platform [79] and with cold trapped-ions [80]. To use the Jarzynski equality in practice, we define a parameter-dependent Hamiltonian for the system of interest $H(\lambda)$, where λ is an externally controlled parameter that can be adjusted according to a fixed protocol. The Jarzynski equality uses work measurements from an ensemble of trajectories as λ is varied to compute the free energy difference between the initial and final equilibrium states. The equality is given by

$$e^{-\beta \Delta F} = \langle e^{-\beta W} \rangle, \tag{1}$$

where $\beta = \frac{1}{k_B T}$ is the inverse temperature T of the system (k_B is Boltzmann's constant) in its initial equilibrium state, ΔF is the free energy difference between the initial and final equilibrium states, W is the work measured for a single trajectory, and $\langle ... \rangle$ represents taking an average over the ensemble of trajectories. Without loss of generality, we assume the initial Hamiltonian of the system $H_i = H(\lambda = 0)$, and the final Hamiltonian $H_f = H(\lambda = 1)$. As shown in Figure 1a, the protocol for varying λ, denoted $\lambda(t)$, occurs over a time τ, which can be defined to be as fast or slow as desired. In general, the faster the protocol, the more trajectories will be required to compute a more accurate estimate of the free energy [81] (see Section III in the SI).

The main challenge in implementing such a procedure is preparing the initial thermal state on the quantum computer. This is a non-trivial problem for which only a handful of algorithms have been proposed, most of which generate circuits that are not feasible (i.e., too large) to run on near-term quantum devices or struggle to scale to large or complex systems [82–86]. A method that is particularly promising for near-term quantum computers produces a Markov chain of sampled pseudo-thermal states, known as minimally entangled typical thermal states (METTS) [87, 88]. Averages of observables over
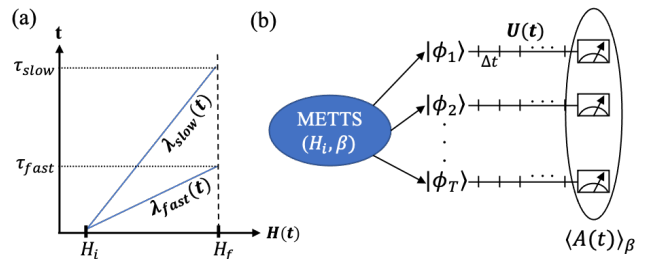

FIG. 1. (a) Schematic diagram depicting how the parameter-dependent Hamiltonian $H(\lambda)$ can be varied over different total times τ. (b) Schematic diagram for the METTS protocol. The protocol requires as input the Hamiltonian and the inverse temperature β of the equilibrium system. The protocol generates a Markov chain of pseudo-thermal states ϕ_i, which can be time-evolved under a separate Hamiltonian, measured, and averaged over to produce the thermal average for some time-dependent observable $A(t)$ at inverse temperature β.

the ensemble of METTS will converge to the true thermal average of the observable with increasing sample size. While initially presented as an method to obtain thermal averages of static observables, METTS can also be used to calculate thermal averages of time-dependent quantities by evolving the METTS in real-time before measurement [89]. Recently, Motta et al. showed how to construct METTS on a quantum computer using the quantum imaginary time evolution (QITE) algorithm [90]. This approach was used to successfully measure thermal averages of both static [90] and dynamic observables [91] on current quantum hardware. Figure 1b shows schematically how measurements of a time-dependent observable $A(t)$ can be averaged over an ensemble of time-evolved METTS for a system with Hamiltonian H_i at inverse temperature β to give the thermal expectation value $\langle A(t) \rangle_\beta$. See Section IV in the SI for more details.

Given an ensemble of pseudo-thermal states generated with the METTS protocol, the initial thermal energy $\langle E_i \rangle$ of the system at inverse temperature β can be measured by averaging over energy measurements of the individual states in the ensemble. Similarly, the final thermal energy $\langle E_f \rangle$ of the system after the $\lambda(t)$ protocol has been implemented can be computed by time-evolving each pseudo-thermal state in the ensemble under the $\lambda(t)$ protocol and averaging over energy measurements of the individual time-evolved states. Now, for closed quantum systems, the work performed in a process is given by the difference in energy of the system before and after the process; therefore, the average thermal energies computed with the METTS ensemble can be used to compute the average work performed over the $\lambda(t)$ protocol, as $\langle W \rangle = \langle E_f \rangle - \langle E_i \rangle$. Note that $\langle W \rangle$ is always an upper bound on the free energy difference due to the reversible work theorem. However, we endeavor to obtain a better approximation to the free energy difference by considering the distribution of individual pseudo-work values derived from the METTS ensemble.

In this framework, we let each METTS in the ensemble correspond to a trajectory. For each trajectory, we compute a pseudo-work value by taking the difference of the measured initial and final energies of the sampled pseudo-thermal state before and after evolving it under the $\lambda(t)$ protocol. While the average over this ensemble of pseudo-work values will converge to the correct value for average work $\langle W \rangle$, the individual values in the ensemble are not necessarily physical work values. This is because the METTS protocol only guarantees accurate averages over the ensemble of METTS. Nevertheless, we show that this distribution can be used in the Jarzynski equality to compute an approximate free energy difference $\Delta\tilde{F}$ as

$$e^{-\beta\Delta\tilde{F}} = \langle e^{-\beta\widetilde{W}} \rangle, \qquad (2)$$

where $\widetilde{W}$ are the individual pseudo-work values computed with the METTS ensemble. In the limit of $\beta \to 0$, this approximation to the free energy difference becomes exact. In the limit of $\beta \to \infty$, $\Delta\tilde{F}$ is exact for $\lambda(t)$ protocols that are adiabatic. For arbitrary β, $\Delta\tilde{F}$ upper bounds the true ΔF for adiabatic $\lambda(t)$ protocols, and is a better approximation to the free energy difference than $\langle W \rangle$ due to Jensen's inequality. See Sections V and VI of the SI for proofs of these statements. For non-adiabatic $\lambda(t)$ protocols, we empirically find that $\Delta F \leq \Delta\tilde{F} \leq \langle W \rangle$ for a range of β's and spin-model Hamiltonians, see Section VII of SI. Plugging the pseudo-work distribution into the Jarzynski equality, therefore provides a very good approximation to the free energy difference for closed quantum systems under certain conditions, and provides a tighter upper bound to the free energy difference than the average work in a broad range of cases. We emphasize that while our algorithm only approximates the free energy difference, it is one of the very few algorithms that can feasibly be performed on near-term quantum computers [19]; and in many instances, this approximation can provide a strict, and even tight, upper bound on the free energy difference.

Algorithm.– We now describe our algorithm, which provides a procedure for obtaining a pseudo-work distribution from non-equilibrium dynamic simulations of a closed quantum system on a quantum computer, which in turn can be used to approximate free energy differences. Pseudocode is shown in Algorithm 1. The algorithm takes as input the parameter-dependent Hamiltonian $H(\lambda)$, the inverse temperature β of the initial system at equilibrium, the protocol $\lambda(t)$ to evolve the parameter from 0 to 1, and the total number of trajectories M. The algorithm generates a pseudo-work distribution by looping over the M trajectories.

For each trajectory, a sub-circuit is generated which prepares the sampled pseudo-thermal state at inverse temperature β ($circ\_TS$), depicted by the red circuit in Figure 2a. According to the METTS protocol, this is accomplished by initializing the qubits into an initial product state (IPS) and evolving it for an imaginary-time $\beta/2$ under the initial Hamiltonian. In this work, we use

---

Algorithm 1: Pseudocode for approximation of free energy differences using METTS with the Jarzynski equality on quantum computers.

Input: $H(\lambda)$, β, $\lambda(t)$, M
Output: Free energy difference
1 work_distribution = [ ]
2 IPS = random_product_state()
   /* Loop over M trajectories   */
3 **for** $m=(0,M)$ **do**
      /* make thermal state preparation circuit   */
4   circ_TS = make_TS_circ(β, $H(\lambda = 0)$, IPS)
      /* get initial state for next trajectory   */
5   circ_M = make_M_circ(circ_TS, m)
6   IPS = collapse(circ_M)
      /* measure inital energy   */
7   circ_E_i = make_E_i_circ($H(\lambda = 0)$, circ_TS)
8   E_i = measure(circ_E_i)
      /* make Hamiltonian evolution circuit   */
9   circ_hamEvol = make_hamEvol_circ($\lambda(t)$, H)
      /* measure final energy   */
10   circ_E_f = make_E_f_circ($H(\lambda = T)$, circ_TS, circ_hamEvol)
11   E_f = measure(circ_E_f)
12   work = E_f - E_i
13   work_distribution.append(work)
14 **return** compute_free_energy(work_distribution, β)

---

the QITE algorithm to implement the imaginary-time evolution, though alternative methods [47, 92] could be substituted. For the first trajectory, IPS is a random product state, while for all subsequent trajectories the new IPS is determined by a projective measurement of the METTS from the previous trajectory.

$circ\_TS$ is then embedded into three separate circuits. The first circuit ($circ\_M$) is used to determine IPS for the next trajectory, depicted by the green circuit in Figure 2a. This circuit collapses the thermal state into a basis which depends on the parity of trajectory m. In order to ensure ergodicity and reduce auto-correlation times, it is helpful to switch between measurement bases throughout sampling [88]. Following the method proposed in Ref. [88] for spin-$\frac{1}{2}$ systems, we measure (i.e., collapse) along the $z-$axis for odd trajectories, while for even trajectories we measure along the $x-$axis.

The second circuit ($circ\_E_i$), measures the expectation value of the initial Hamiltonian $H(\lambda = 0)$ in the pseudo-thermal state to give the initial energy. Finally, the third circuit ($circ\_E_f$) measures the final energy. To generate this circuit, a sub-circuit ($circ\_hamEvol$) is first created to evolve the system under the time-dependent Hamiltonian according to the $\lambda(t)$ protocol. In this work, we use a recently proposed method for implementing the real-time evolution with short, constant-depth circuits, which works for a special subset of one-dimensional systems [44]. However, more general methods, such as standard Trotterization or variational techniques [93, 94], can be substituted. This sub-circuit is appended to ($circ\_TS$) to generate the time-evolved pseudo-thermal state. The

final energy is obtained by measuring the expectation value of the final Hamiltonian $H(\lambda = 1)$ in this state. The circuits for measuring initial and final energies are depicted by the blue circuits in Figure 2a. The difference between these energies gives the pseudo-work for the given trajectory. The free energy difference can then be approximated by plugging the pseudo-work ensemble into Eq. (2).
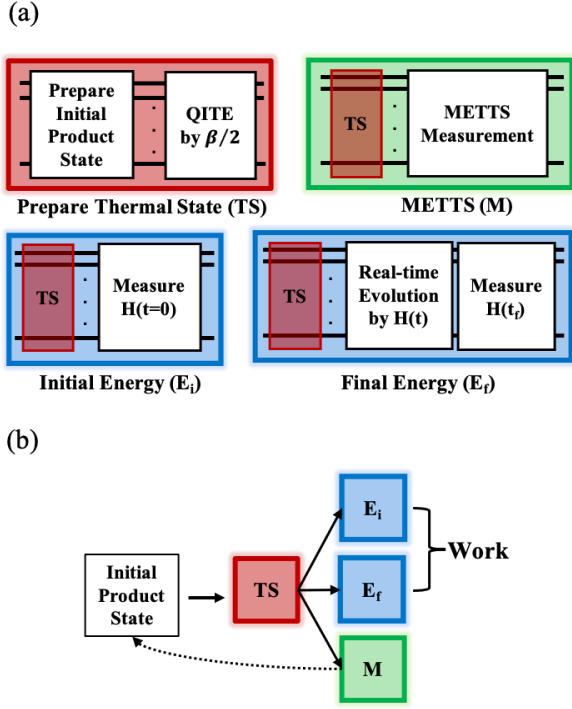
(a)

(b)

FIG. 2. Circuits generated and workflow diagram for the algorithm. (a) Quantum circuit diagrams for the thermal state preparation sub-circuit (red), which is used in three separate circuits for measuring the initial and final energies (blue) as well as measuring the initial product state for the subsequent trajectory (green). (b) Workflow diagram depicting how the circuits above are integrated to produce a pseudo-work distribution.

Figure 2b shows how a pseudo-work value is derived from the three main circuits for each trajectory and how measurement of the M circuit from the previous trajectory provides input to the TS sub-circuit for the next trajectory. Note that the first few trajectories should be discarded as "warm-up" values [87].

Results.– We demonstrate our algorithm on real quantum hardware with a 2- and 3-qubit TFIM as a proof-of-concept. The Hamiltonian is defined as

$$H(\lambda) = J_z \sum_{i=1}^{N-1} \sigma_i^z \sigma_{i+1}^z + (1 + \frac{\lambda(t)}{2})h_x \sum_{i=1}^{N} \sigma_i^x, \qquad (3)$$

where N is the number of spins in the system, J_z is the strength of the exchange interaction between pairs of nearest neighbor spins, h_x is the strength of the trans-
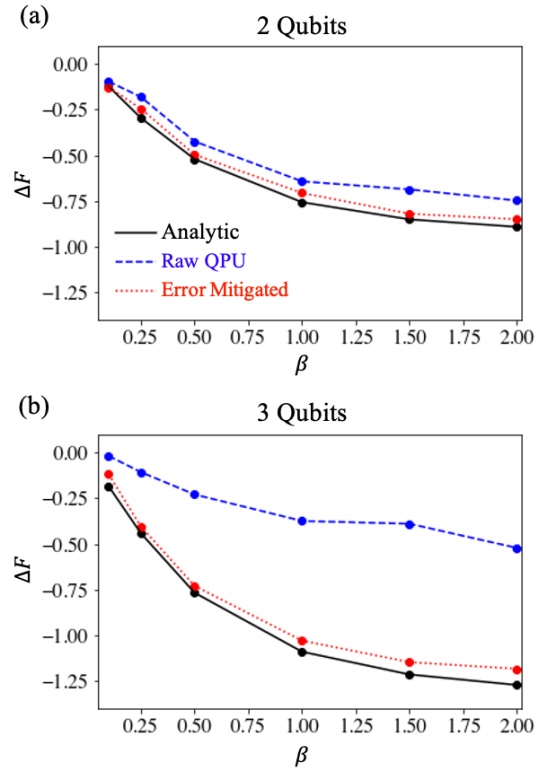

FIG. 3. Approximate free energy differences ($\Delta \widetilde{F}$) for 2- and 3-qubit systems initialized at various inverse temperatures β performed on an IBM quantum processing unit (QPU). The solid black line gives the analytically computed values (ΔF) for reference. The blue dashed lines show raw results from the QPU, while the red dotted lines show these results after error mitigation has been performed.

verse magnetic field, and σ_i^α is the α-Pauli operator acting on spin i. The system starts in thermal equilibrium at an inverse temperature β with an initial Hamiltonian $H_i = H(\lambda = 0) = J_z \sum_i \sigma_i^z \sigma_{i+1}^z + h_x \sum_i \sigma_i^x$. The parameter λ is then linearly increased from 0 to 1 over a total time τ, resulting in a system with a final Hamiltonian $H_f = H(\lambda = 1) = J_z \sum_i \sigma_i^z \sigma_{i+1}^z + 1.5h_x \sum_i \sigma_i^x$. We set $J_z = 1$, $h_x = 1$, and $\tau = 10$, and set the number of trajectories $M = 100$ for the 2-qubit system and $M = 300$ for the 3-qubit system.

Figure 3 shows the approximate free energy differences at various inverse temperatures β computed using our algorithm on the IBM quantum processing unit (QPU) "ibmq_toronto" for a 2-qubit system (a) and a 3-qubit system (b). The black solid lines show the analytically computed free energy differences, which are possible to compute due to the small size of our systems. The blue dashed lines show raw results from the QPU. The quantum circuits for the 3-qubit simulations are significantly larger than those for the 2-qubit simulations, and thus accumulate more error due to hardware noise. This explains why the QPU results for the 2-qubit system are significantly closer to the ground truth than those for the 3-qubit system. To ameliorate this systematic noise, we

implement two error mitigation techniques. The first is known as zero-noise extrapolation (ZNE) [95, 96], which combats noise arising from two-qubit entangling gates, which are currently one of the largest sources of error on near-term quantum devices. We pair ZNE with a second error mitigation technique to combat readout error, which is error derived from the measurement operation. See Section VIII of the SI for more details on error mitigation. The QPU results after error mitigation are shown in the red dotted lines. The error mitigated results are in excellent agreement with the analytic results for both system sizes, demonstrating the ability of the two error mitigation techniques to combat major contributions to noise on the quantum computer.

In addition to the systematic errors derived from noisy near-term quantum devices, another source of error stems from the using the QITE algorithm to approximate the imaginary time evolution required to generate the METTS. The size of this error depends on the step-size $\Delta\beta$ used to construct the QITE circuits for thermal state preparation at inverse temperature β. This error can systematically be made smaller by decreasing $\Delta\beta$ at the expense of complexity in building the quantum circuit. In general, Trotter error will be another source of error, which arises from the most commonly used approach to generate the real-time evolution operator used to evolve the system as λ is varied from 0 to 1. However, we were able to make this negligible using techniques developed in [44], which apply to the real-time evolution of TFIMs. See Section IX of the SI for more details.

Conclusion.–We have introduced an algorithm for computing free energy differences of quantum systems on quantum computers using fluctuation relations. We demonstrated our algorithm on IBM's quantum processor for the TFIM, resulting in free energy differences in excellent agreement with the ground truth after applying two simple error mitigation techniques. The main bot-tleneck to using our algorithm for larger systems is the limit on the size of quantum circuits that is feasible to execute on currently available quantum hardware. The imaginary- and real-time evolution components of our algorithm are the largest contributors to circuit depths. Thus, targeting more relevant systems with our algorithm can be addressed by developing new, shorter-depth implementations for imaginary- and real-time evolution. Due to the modularity of our algorithm, such implementations can easily be substituted in as they become available. Simultaneously, new methods for quantum error mitigation, as well as continued improvements made to quantum processors will further extend the depths of circuits that are feasible to execute. Because of the significant progress in these areas over the last few years [44–50] we anticipate that our algorithm will become increasingly important as a means to compute free energy differences in scientifically relevant systems as quantum computers become more powerful.

[1] D. A. Kofke and D. Frenkel, Perspective: free energies and phase equilibria, in *Handbook of Materials Modeling* (Springer, 2005) pp. 683–705.

[2] R. Fishman and S. Liu, Free energy and phase diagram of chromium alloys, Physical Review B **48**, 3820 (1993).

[3] S. Franz and G. Parisi, Phase diagram of coupled glassy systems: A mean-field study, Physical review letters **79**, 2486 (1997).

[4] C. Cazorla, D. Alfe, and M. J. Gillan, Constraints on the phase diagram of molybdenum from first-principles free-energy calculations, Physical Review B **85**, 064113 (2012).

[5] C. Cazorla and J. Íniguez, Insights into the phase diagram of bismuth ferrite from quasiharmonic free-energy calculations, Physical Review B **88**, 214430 (2013).

[6] C. Chipot and A. Pohorille, *Free Energy Calculations: Theory and Applications in Chemistry and Biology*, Vol. 86 (Springer, New York, 2007).

[7] M. R. Reddy and M. D. Erion, *Free energy calculations in rational drug design* (Springer Science & Business Media, 2001).

[8] M. R. Shirts, D. L. Mobley, and S. P. Brown, *Free-energy calculations in structure-based drug design* (Cambridge University Press, New York, 2010) pp. 61–86.

[9] M. Rami Reddy, C. Ravikumar Reddy, R. S Rathore, M. D Erion, P. Aparoy, R. Nageswara Reddy, and P. Reddanna, Free energy calculations to estimate ligand-binding affinities in structure-based drug design, Current pharmaceutical design **20**, 3323 (2014).

[10] R. Abel, L. Wang, E. D. Harder, B. Berne, and R. A. Friesner, Advancing drug discovery through enhanced free energy calculations, Accounts of chemical research **50**, 1625 (2017).

[11] B. J. Williams-Noonan, E. Yuriev, and D. K. Chalmers, Free energy methods in drug design: Prospects of "alchemical perturbation" in medicinal chemistry: miniperspective, Journal of medicinal chemistry **61**, 638 (2018).

[12] D. Frenkel and B. Smit, *Understanding molecular simu-*

lation: from algorithms to applications, Vol. 1 (Elsevier, 2001).

[13] M. Tuckerman, *Statistical mechanics: theory and molecular simulation* (Oxford University Press, New York, 2010).

[14] A. Pohorille, C. Jarzynski, and C. Chipot, Good practices in free-energy calculations, The Journal of Physical Chemistry B **114**, 10235 (2010).

[15] A. Barducci, G. Bussi, and M. Parrinello, Well-tempered metadynamics: a smoothly converging and tunable free-energy method, Physical review letters **100**, 020603 (2008).

[16] O. Valsson and M. Parrinello, Variational approach to enhanced sampling and free energy calculations, Physical review letters **113**, 090601 (2014).

[17] M. Troyer, S. Wessel, and F. Alet, Flat histogram methods for quantum systems: algorithms to overcome tunneling problems and calculate the free energy, Physical review letters **90**, 120201 (2003).

[18] G. Piccini and M. Parrinello, Accurate quantum chemical free energies at affordable cost, The journal of physical chemistry letters **10**, 3727 (2019).

[19] A. Francis, D. Zhu, C. Huerta Alderete, S. Johri, X. Xiao, J. K. Freericks, C. Monroe, N. M. Linke, and A. F. Kemper, Many-body thermodynamics on quantum computers via partition function zeros, Science Advances **7**, eabf2447 (2021).

[20] See Supplemental Material at ** for further explanations, simulations, and proofs of claims made in the main text.

[21] M. Schüler, C. Renk, and T. Wehling, Variational exact diagonalization method for anderson impurity models, Physical Review B **91**, 235142 (2015).

[22] A. Laio and M. Parrinello, Escaping free-energy minima, Proceedings of the National Academy of Sciences **99**, 12562 (2002).

[23] G. M. Torrie and J. P. Valleau, Nonphysical sampling distributions in monte carlo free-energy estimation: Umbrella sampling, Journal of Computational Physics **23**, 187 (1977).

[24] F. Wang and D. P. Landau, Efficient, multiple-range random walk algorithm to calculate the density of states, Physical review letters **86**, 2050 (2001).

[25] M. Esposito, U. Harbola, and S. Mukamel, Nonequilibrium fluctuations, fluctuation theorems, and counting statistics in quantum systems, Reviews of modern physics **81**, 1665 (2009).

[26] M. Campisi, P. Hänggi, and P. Talkner, Colloquium: Quantum fluctuation relations: Foundations and applications, Reviews of Modern Physics **83**, 771 (2011).

[27] C. Jarzynski, Equilibrium free-energy differences from nonequilibrium measurements: A master-equation approach, Physical Review E **56**, 5018 (1997).

[28] C. Jarzynski, Nonequilibrium equality for free energy differences, Physical Review Letters **78**, 2690 (1997).

[29] R. P. Feynman, Simulating physics with computers, Int. J. Theor. Phys. **21**, 467 (1982).

[30] S. Lloyd, Universal quantum simulators, Science **273**, 1073 (1996).

[31] D. S. Abrams and S. Lloyd, Simulation of many-body Fermi systems on a universal quantum computer, Phys. Rev. Lett. **79**, 2586 (1997).

[32] C. Zalka, Simulating quantum systems on a quantum computer, Proc. R. Soc. A **454**, 313 (1998).

[33] R. Barends, L. Lamata, J. Kelly, L. García-Álvarez, A. G. Fowler, A. Megrant, E. Jeffrey, T. C. White, D. Sank, J. Y. Mutus, *et al.*, Digital quantum simulation of fermionic models with a superconducting circuit, Nature communications **6**, 1 (2015).

[34] N. Klco, E. F. Dumitrescu, A. J. McCaskey, T. D. Morris, R. C. Pooser, M. Sanz, E. Solano, P. Lougovski, and M. J. Savage, Quantum-classical computation of schwinger model dynamics using quantum computers, Physical Review A **98**, 032331 (2018).

[35] A. Zhukov, S. Remizov, W. Pogosov, and Y. E. Lozovik, Algorithmic simulation of far-from-equilibrium dynamics using quantum computer, Quantum Information Processing **17**, 1 (2018).

[36] H. Lamm and S. Lawrence, Simulation of nonequilibrium dynamics on a quantum computer, Physical review letters **121**, 170501 (2018).

[37] A. Cervera-Lierta, Exact ising model simulation on a quantum computer, Quantum **2**, 114 (2018).

[38] A. Smith, M. Kim, F. Pollmann, and J. Knolle, Simulating quantum many-body dynamics on a current digital quantum computer, npj Quantum Information **5**, 1 (2019).

[39] L. Bassman, K. Liu, A. Krishnamoorthy, T. Linker, Y. Geng, D. Shebib, S. Fukushima, F. Shimojo, R. K. Kalia, A. Nakano, *et al.*, Towards simulation of the dynamics of materials on quantum computers, Physical Review B **101**, 184305 (2020).

[40] B. Fauseweh and J.-X. Zhu, Digital quantum simulation of non-equilibrium quantum many-body systems, Quantum Information Processing **20**, 1 (2021).

[41] A. Chiesa, F. Tacchino, M. Grossi, P. Santini, I. Tavernelli, D. Gerace, and S. Carretta, Quantum hardware simulating four-dimensional inelastic neutron scattering, Nature Physics **15**, 455 (2019).

[42] A. Francis, J. Freericks, and A. Kemper, Quantum computation of magnon spectra, Physical Review B **101**, 014411 (2020).

[43] X.-Y. Guo, Z.-Y. Ge, H. Li, Z. Wang, Y.-R. Zhang, P. Song, Z. Xiang, X. Song, Y. Jin, L. Lu, *et al.*, Observation of bloch oscillations and wannier-stark localization on a superconducting quantum processor, npj Quantum Information **7**, 1 (2021).

[44] L. Bassman, R. Van Beeumen, E. Younis, E. Smith, C. Iancu, and W. A. de Jong, Constant-depth circuits for dynamic simulations of materials on quantum computers, Materials Theory **6**, 1 (2022).

[45] J.-L. Ville, A. Morvan, A. Hashim, R. K. Naik, M. Lu, B. Mitchell, J.-M. Kreikebaum, K. P. O'Brien, J. J. Wallman, I. Hincks, *et al.*, Leveraging randomized compiling for the qite algorithm, arXiv preprint arXiv:2104.08785 (2021).

[46] S.-H. Lin, R. Dilip, A. G. Green, A. Smith, and F. Pollmann, Real-and imaginary-time evolution with compressed quantum circuits, PRX Quantum **2**, 010342 (2021).

[47] D. Camps and R. Van Beeumen, Fable: Fast approximate quantum circuits for block-encodings, arXiv preprint arXiv:2205.00081 (2022).

[48] B. Koczor, Exponential error suppression for near-term quantum devices, Physical Review X **11**, 031057 (2021).

[49] P. Czarnik, A. Arrasmith, P. J. Coles, and L. Cincio, Error mitigation with clifford quantum-circuit data, Quantum **5**, 592 (2021).

[50] F. Tacchino, A. Chiesa, S. Carretta, and D. Gerace, Quantum computers as universal quantum simulators: state-of-the-art and perspectives, Advanced Quantum Technologies **3**, 1900052 (2020).

[51] P. A. Lee, N. Nagaosa, and X.-G. Wen, Doping a mott insulator: Physics of high-temperature superconductivity, Reviews of modern physics **78**, 17 (2006).

[52] M. Imada, A. Fujimori, and Y. Tokura, Metal-insulator transitions, Reviews of modern physics **70**, 1039 (1998).

[53] J. Voit, One-dimensional fermi liquids, Reports on Progress in Physics **58**, 977 (1995).

[54] L. Tarruell and L. Sanchez-Palencia, Quantum simulation of the hubbard model with ultracold fermions in optical lattices, Comptes Rendus Physique **19**, 365 (2018).

[55] N. Brunner, N. Linden, S. Popescu, and P. Skrzypczyk, Virtual qubits, virtual temperatures, and the foundations of thermodynamics, Physical Review E **85**, 051117 (2012).

[56] L. P. García-Pintos, A. Hamma, and A. Del Campo, Fluctuations in extractable work bound the charging power of quantum batteries, Physical Review Letters **125**, 040601 (2020).

[57] B. Nagler, S. Barbosa, J. Koch, G. Orso, and A. Widera, Observing the loss and revival of long-range phase coherence through disorder quenches, Proceedings of the National Academy of Sciences **119**, e2111078118 (2022).

[58] G. Hummer and A. Szabo, Free energy reconstruction from nonequilibrium single-molecule pulling experiments, Proceedings of the National Academy of Sciences **98**, 3658 (2001).

[59] J. Liphardt, S. Dumont, S. B. Smith, I. Tinoco, and C. Bustamante, Equilibrium information from nonequilibrium measurements in an experimental test of jarzynski's equality, Science **296**, 1832 (2002).

[60] F. Douarche, S. Ciliberto, A. Petrosyan, and I. Rabbiosi, An experimental test of the jarzynski equality in a mechanical experiment, EPL (Europhysics Letters) **70**, 593 (2005).

[61] N. C. Harris, Y. Song, and C.-H. Kiang, Experimental free energy surface reconstruction from single-molecule force spectroscopy using jarzynski's equality, Physical review letters **99**, 068101 (2007).

[62] O.-P. Saira, Y. Yoon, T. Tanttu, M. Möttönen, D. Averin, and J. P. Pekola, Test of the jarzynski and crooks fluctuation relations in an electronic system, Physical review letters **109**, 180601 (2012).

[63] S. Toyabe, T. Sagawa, M. Ueda, E. Muneyuki, and M. Sano, Experimental demonstration of information-to-energy conversion and validation of the generalized jarzynski equality, Nature physics **6**, 988 (2010).

[64] H. Tasaki, Jarzynski relations for quantum systems and some applications, arXiv preprint cond-mat/0009244 (2000).

[65] J. Kurchan, A quantum fluctuation theorem, arXiv preprint cond-mat/0007360 (2000).

[66] B. Piechocinska, Information erasure, Physical Review A **61**, 062314 (2000).

[67] S. Mukamel, Quantum extension of the jarzynski relation: Analogy with stochastic dephasing, Physical review letters **90**, 170604 (2003).

[68] T. Monnai, Unified treatment of the quantum fluctuation theorem and the jarzynski equality in terms of microscopic reversibility, Physical Review E **72**, 027102 (2005).

[69] S. Yukawa, A quantum analogue of the jarzynski equality, Journal of the Physical Society of Japan **69**, 2367 (2000).

[70] V. Chernyak and S. Mukamel, Effect of quantum collapse on the distribution of work in driven single molecules, Physical review letters **93**, 048302 (2004).

[71] W. De Roeck and C. Maes, Quantum version of free-energy–irreversible-work relations, Physical Review E **69**, 026115 (2004).

[72] G. E. Crooks, On the jarzynski relation for dissipative quantum dynamics, Journal of Statistical Mechanics: Theory and Experiment **2008**, P10023 (2008).

[73] M. Campisi, P. Talkner, and P. Hänggi, Fluctuation theorem for arbitrary open quantum systems, Physical review letters **102**, 210401 (2009).

[74] V. A. Ngo and S. Haas, Demonstration of jarzynski's equality in open quantum systems using a stepwise pulling protocol, Physical Review E **86**, 031127 (2012).

[75] G. B. Cuetara, A. Engel, and M. Esposito, Stochastic thermodynamics of rapidly driven systems, New journal of physics **17**, 055002 (2015).

[76] B. P. Venkatesh, G. Watanabe, and P. Talkner, Quantum fluctuation theorems and power measurements, New Journal of Physics **17**, 075018 (2015).

[77] A. Sone and S. Deffner, Jarzynski equality for conditional stochastic work, Journal of Statistical Physics **183**, 1 (2021).

[78] G. Huber, F. Schmidt-Kaler, S. Deffner, and E. Lutz, Employing trapped cold ions to verify the quantum jarzynski equality, Physical review letters **101**, 070403 (2008).

[79] T. B. Batalhão, A. M. Souza, L. Mazzola, R. Auccaise, R. S. Sarthour, I. S. Oliveira, J. Goold, G. De Chiara, M. Paternostro, and R. M. Serra, Experimental reconstruction of work distribution and study of fluctuation relations in a closed quantum system, Physical review letters **113**, 140601 (2014).

[80] S. An, J.-N. Zhang, M. Um, D. Lv, Y. Lu, J. Zhang, Z.-Q. Yin, H. Quan, and K. Kim, Experimental test of the quantum jarzynski equality with a trapped-ion system, Nature Physics **11**, 193 (2015).

[81] H. Oberhofer, C. Dellago, and P. L. Geissler, Biased sampling of nonequilibrium trajectories: Can fast switching simulations outperform conventional free energy calculation methods?, The Journal of Physical Chemistry B **109**, 6902 (2005).

[82] D. Poulin and P. Wocjan, Sampling from the thermal quantum gibbs state and evaluating partition functions with a quantum computer, Physical review letters **103**, 220502 (2009).

[83] A. Riera, C. Gogolin, and J. Eisert, Thermalization in nature and on a quantum computer, Physical review letters **108**, 080402 (2012).

[84] G. Verdon, J. Marks, S. Nanda, S. Leichenauer, and J. Hidary, Quantum hamiltonian-based models and the variational quantum thermalizer algorithm, arXiv preprint arXiv:1910.02071 (2019).

[85] J. Wu and T. H. Hsieh, Variational thermal quantum simulation via thermofield double states, Physical review letters **123**, 220502 (2019).

[86] D. Zhu, S. Johri, N. Linke, K. Landsman, C. H. Alderete, N. Nguyen, A. Matsuura, T. Hsieh, and C. Monroe, Generation of thermofield double states and critical ground states with a quantum computer, Proceedings of the National Academy of Sciences **117**, 25402 (2020).

[87] S. R. White, Minimally entangled typical quantum states

at finite temperature, Physical review letters **102**, 190601 (2009).

[88] E. Stoudenmire and S. R. White, Minimally entangled typical thermal state algorithms, New Journal of Physics **12**, 055026 (2010).

[89] L. Bonnes, F. H. Essler, and A. M. Läuchli, "light-cone" dynamics after quantum quenches in spin chains, Physical review letters **113**, 187203 (2014).

[90] M. Motta, C. Sun, A. T. Tan, M. J. O'Rourke, E. Ye, A. J. Minnich, F. G. Brandão, and G. K.-L. Chan, Determining eigenstates and thermal states on a quantum computer using quantum imaginary time evolution, Nature Physics **16**, 205 (2020).

[91] S.-N. Sun, M. Motta, R. N. Tazhigulov, A. T. Tan, G. K.-L. Chan, and A. J. Minnich, Quantum computation of finite-temperature static and dynamical properties of spin systems using quantum imaginary time evolution, PRX Quantum **2**, 010317 (2021).

[92] R. M. Gingrich and C. P. Williams, Non-unitary proba-

bilistic quantum computing, in *Proceedings of the Winter International Synposium on Information and Communication Technologies*, WISICT '04 (Trinity College Dublin, 2004) p. 1–6.

[93] C. Cirstoiu, Z. Holmes, J. Iosue, L. Cincio, P. J. Coles, and A. Sornborger, Variational fast forwarding for quantum simulation beyond the coherence time, npj Quantum Information **6**, 1 (2020).

[94] S. Barison, F. Vicentini, and G. Carleo, An efficient quantum algorithm for the time evolution of parameterized circuits, Quantum **5**, 512 (2021).

[95] K. Temme, S. Bravyi, and J. M. Gambetta, Error mitigation for short-depth quantum circuits, Physical review letters **119**, 180509 (2017).

[96] Y. Li and S. C. Benjamin, Efficient variational quantum simulator incorporating active error minimization, Physical Review X **7**, 021050 (2017).